ELSEVIER

Magnetic Resonance Materials in Physics, Biology and Medicine 8 (1999) 207–213

MAGMA

Magnetic Resonance Materials in Physics, Biology and Medicine

www.elsevier.com/locate/magma

'NC100150', a preparation of iron oxide nanoparticles ideal for positive-contrast MR angiography

Kenneth E. Kellar [a,*], Dennis K. Fujii [a], Wolfgang H.H. Gunther [a], Karen Briley-Sæbø [b], Marga Spiller [c], Seymour H. Koenig [d,e]

[a] *Nycomed Amersham Imaging, 466 Devon Park Drive, P. O. Box 6630, Wayne, PA 19087-8630, USA*
[b] *Nycomed Imaging AS, Nycoveien 1-2, P.O. Box 4220 Torshov, N-0401 Oslo, Norway*
[c] *Department of Radiology, New York Medical College, Valhalla, NY 10598, USA*
[d] *Relaxometry Inc., P. O. Box 760, Mahopac, NY 10541, USA*
[e] *Department of Medical Information Sciences, University of Illinois, Urbana, IL 61801, USA*

Abstract

A laboratory-scale synthesis of NC100150 (iron oxide particles with an oxidized starch coating) was characterized by magnetization measurements (vibrating sample magnetometry, VSM), relaxometry ($1/T_1$ NMRD profiles and $1/T_2$ at 10 and 20 MHz), and dynamic light scattering (photon correlation spectroscopy, PCS). The results were related to give a self-consistent physical description of the particles: a water-impenetrable part making up 12% of the total particle volume, 82% of this volume consisting of an iron oxide core and the remaining 18% consisting of an oxidized starch rind; and, a water-penetrable part making up 88% of the total particle volume, consisting of oxidized starch polymers and entrained water molecules. Relating the magnetization to the relaxometry results required that the oxidized starch coating slows the diffusivity of solvent water molecules in the vicinity of the iron oxide cores. The effect of the organic coating on water diffusivity, not previously considered in the application of relaxation theory to iron oxide nanoparticles, is supported by the much greater (factor of about 2) diameter obtained from the dynamic light scattering measurements in comparison to that obtained from the magnetization measurements. The present work shows that three physical techniques—VSM, relaxometry, and PCS—are needed for properly assessing iron oxide nanoparticles for use as contrast agents for magnetic resonance angiography (MRA). It is also shown that NC100150 has a narrow range of diameters and the smallest value of r_2/r_1 reported to date, an asset for MRA.

Keywords: Iron oxide nanoparticles; Magnetization data; NMRD profiles; Outer-sphere relaxation

1. Introduction

Monocrystalline iron oxide nanoparticles, with an organic polymer coating to increase solubility and stability, are widely used as negative (or T_2) contrast agents for MRI, particularly for imaging the liver [1]. In the liver, the particles are taken up by Kupffer cells, which then act like much larger magnetic particles: T_2-shortening results from the diffusion of liver water molecules in the 'outer sphere' environment of the Kupffer cells. For nanoparticles of a given magnetochemical formulation, their efficacy as negative agents depends on the total amount of particles taken up by the Kupffer cells and is relatively insensitive to their size distribution. More recently, however, iron oxide particles have been investigated as positive contrast agents for MR angiography (MRA) [2], an application which depends on T_1-shortening in the vasculature. Quite different from their *collective* behavior as negative contrast agents, their efficacy as positive agents is directly related to T_1-reduction by *individual* particles, which places stringent demands on the physical characteristics of the nanoparticles. To optimize their utility for MRA, the appropriate magnetic material (usually magnetite or maghemite) must be synthesized reproducibly, and the core size of the iron oxide nanocrystals and its variability must be carefully controlled.

* Corresponding author. Tel.: + 1-610-225-4338; fax: + 1-610-225-4416.

E-mail address: kenneth.kellar@us.nycomed-amersham.com (K.E. Kellar)

Defining nanoparticle relaxivities as $r_i = (1/T_i - 1/T_{iW})/[Fe]$, where $i = 1, 2$ and $1/T_{iW}$ is the background contribution of water, theory indicates that, in the MRA magnetic field-range, the optimal utility of these particles as positive contrast agents is very sensitive to the ratio r_2/r_1 [3]. This ratio, in turn, is a function of the diameter of the iron oxide, agglomeration of the solute nanoparticles, and magnetic field strength. A ratio near 2 at 20 MHz and body temperature is necessary; too low a value gives little contrast enhancement and too large a value diminishes the signal intensity adversely [3]. A ratio of about 1.6–1.7 is ideal for the use of these nanoparticles at MRA field strengths (> 0.5 T), since r_1 decreases with increasing field strength more strongly the higher the value of this ratio [3]. Consequently, it necessary to have reproducible preparations of controlled and relatively monodisperse iron oxide diameters. In the current work, we have prepared maghemite (γ-Fe_2O_3) nanoparticles, coated with an oxidized starch, having an r_2/r_1 of 1.6–1.7, called NC100150.

Although preparing monodisperse iron oxide cores of the appropriate size is essential to preparing an agent with the proper relaxivities, the organic coating may also influence the relaxivities due to its effect on the diffusion of nearby water molecules. Therefore, in order to properly characterize the MRA efficacy, it is necessary to characterize NC100150 using a physical property that is not sensitive to the organic coating: the measurement of magnetization as a function of magnetic field strength [4]. Using this thermodynamic technique, the core diameter d and magnetic moment μ (obtained with this technique as volume-average quantities) are obtained without any influence from the oxidized starch coating. Using relaxation theory [3], the magnetization data can be reconciled with relaxometry data, which includes $1/T_1$ NMRD profiles and the measurement of the r_2/r_1 ratio at 10 and 20 MHz. The relaxometry results are not thermodynamic, but depend on the dynamics of the solvent water molecules near the nanoparticles, which can be characterized by a diffusivity D. The approach used here is to treat D as an adjustable parameter, rather than to assume its value to be that of pure water, D_W (as is adequate for small paramagnetic chelates), while keeping d and μ fixed at the values obtained from the magnetization results. Finally, photon correlation spectroscopy (PCS), which gives a measure of the translational diffusion constant of an entire composite nanoparticle [5], is used to infer the extent to which water molecules near solute become entrained in the starch structure by viscosity [6], altering water dynamics in this region. Using these three physical measurements, we confirm that the organic coating must be considered in the interpretation of relaxometry data and that we have prepared maghemite nanoparticles with a narrow range of diameters and the smallest value of r_2/r_1 reported to date.

2. Materials and methods

2.1. Synthesis of NC100150

Soluble potato starch (50 g/l; Sigma S-2630) is dissolved in 850 ml of boiling deionized water and then cooled in a 55°C water bath. A 2:1 molar ratio of ferric to ferrous chloride (9.0 grams $FeCl_3 \cdot 6H_2O$ + 3.3 grams $FeCl_2 \cdot 4H_2O$) is then dissolved in 50 ml of deionized water and stirred into the starch solution. A nonmagnetic iron hydroxide precipitate is then formed by adding 50 ml of concentrated ammonium hydroxide, while stirring. The water bath is slowly heated to 90°C, taking 90 min, and maintained there for another 80 min with constant stirring. The result is a black slurry, ostensibly a mixture of magnetite (Fe_3O_4) and maghemite. This is allowed to gel overnight at 5°C, and then washed repeatedly with cold deionized water (suspend gel in water, settle, and decant) until the pH is in the range 6–8. The gel is allowed to settle, the majority of the water is then aspirated, and the gel recovered. The iron concentration of the gel (mg/g Fe of gel) is determined using a Ferrozine-based colorimetric assay (Sigma, 565-C) after acid hydrolysis of the gel.

The iron oxide particles are released from the starch by oxidizing with sodium hypochlorite (Aldrich, 29,930-5; available $Cl \geq 4\%$). Typically 0.4 ml of a sodium hypochlorite solution is added for each gram of gel (containing 2.5 mg Fe), the solution heated to 70°C for 45 min, and the reaction quenched by adding urea (0.16 ml of 8 M/g urea of gel). The resulting dark reddish-brown solution is filtered (0.8 μm) to remove small particles of unreacted starch, exhaustively diafiltered against deionized water (100 kDa cutoff), and concentrated to 5–30 mg/ml Fe. The sample is again filtered (0.1 μm) and stored at 5°C. The yield of iron, 70%, is typical for this process. There was no free iron or starch in the solutions used, as determined by ultrafiltration or ultracentrifugation after removal of the nanoparticles. Consequently, the final iron oxide crystals retain a coating of oxidized starch polymers, but the organization of the starch on the surface is not known. However, as will be discussed, the polymers must be organized to create a barrier to water diffusion about 0.2 nm thick on the surface of the core, and to lower the diffusivity of the water some distance beyond. Because of the oxidative nature of hypochlorite treatment, the iron oxide particles are expected be the ferric oxide maghemite, consistent with the magnetization measurements (see below). These maghemite nanoparticles, with coatings of oxidized starch polymer, are 'NC100150'.

2.2. MION-46L

MION-46L in sodium citrate buffer, nominally 8.0 mg/ml in iron, was purchased from The Center for Molecular Imaging Research (Massachusetts General Hospital, Boston, MA; price and properties available at the time on their web page). Many physical characteristics of MION-46, an earlier preparation of MION-46L, have been reported previously [7]. Only magnetization measurements were performed here for the MION-46L solution. A more detailed investigation of MION-46L, including relaxometry and PCS measurements, will be reported elsewhere.

2.3. Sample preparation

For magnetization measurements, the NC100150 solution from the synthesis was used directly (2.57 mg/ml Fe), and for the MION-46L, the purchased solution was used as is (7.18 mg/ml Fe). For $1/T_1$ NMRD measurements and the two $1/T_2$ measurements, the original NC100150 solution was diluted with distilled water to 15.0 μg/ml Fe. The iron concentrations of the samples were determined by ICP analysis (Quantitative Technologies, Inc., Whitehouse, NJ). For PCS, an aliquot of the original NC100150 solution was diluted with filtered (0.1 μm) distilled water, to minimize multiple photon scattering, to a concentration that still gave sufficient scattering intensity to allow for accurate measurements.

2.4. Optical characterization

Photon correlation spectroscopy (PCS) measures the Doppler-broadening of scattered, highly monochromatic, laser radiation that results from translational Brownian motion [5] of (here) composite solute nanoparticles. This broadening can be related directly to a solute translational diffusion constant D_F, in terms of the frequency of the radiation, the scattering angle, and the refractive index of the solution. From Stokes' law, $D_F = kT/3\pi\eta d_{PCS}$, where k is the Boltzmann constant, T the absolute temperature, η the solvent viscosity, and d_{PCS} the 'hydrodynamic' diameter of a solute particle, assumed spherical. For coated nanoparticles, d_{PCS} includes a contribution from the effective radius of gyration of the attached starch polymers, which defines a volume beyond the core in which the associated water can be regarded as part of the diffusive mass of the nanoparticle [6]. The attached oxidized starch polymers can be regarded as flexible, and such flexible polymers have long been known to be very highly hydrated; the effective radius of gyration can as large as 80% of the usual radius of gyration [6]. Although much solvent is dynamically entrained within the region of the polymeric coating by viscosity, these water molecules are in rapid exchange with the bulk solvent, a requirement for high relaxivity.

Measurements were made, at 20°C, using a Brookhaven light scattering spectrophotometer (BI-9000AT; Brookhaven Instruments Corporation, Holtsville, NY) equipped with a 150 mW laser (514 nm). The scattering angle was 90°, and the data were analyzed by the method of cumulants [5].

2.5. Magnetic characterization

To characterize the magnetic properties of iron oxide nanoparticles of the size-range of NC100150, both magnetization and solvent proton relaxation must be measured in the low- and high-field regimes. These regimes are defined by the value of x, the ratio of the magnetic energy of a nanoparticle compared to its thermal energy: $x = \mu B_0/kT$, where B_0 is the applied static field. In the low-field range, $x \ll 1$, and the magnetic energy is not sufficient to significantly alter the orientational distribution of the moments of the solute particles. The response of a sample to B_0, called the 'Curie magnetization', is then given by an average of the interaction energy of μ and B_0 over the unperturbed distribution. In the high-field range, $x \gg 1$, and the magnetic energy of the solute particles far exceeds their thermal energy; the magnetic moments of individual particles progressively align parallel to B_0. For the iron oxide particles considered here, the condition $x \approx 1$ occurs near 0.2 T, somewhat below the usual MRI range.

2.5.1. Magnetization measurements

The macroscopic magnetic moment of a sample was measured at 25°C, as a function of B_0, using a vibrating sample magnetometer (VSM, Molspin Ltd., UK). The instrument was calibrated using Ni(I) and Ni(II) standards, for which the macroscopic moment is known over the field strength range of the instrument (from -1 to 1 T). Using a solution with the appropriate iron concentration, the samples were made comparable in size, geometry, and magnetic moment to the standards. The result, when normalized to sample volume, is the field-dependent (macroscopic) magnetization M.

The form of the magnetization curve between the low-field Curie range and high-field near-saturation range is described by the Brillouin function, which is linear for $x \ll 1$, is ≈ 0.5 for $x = 2$, and approaches unity as $1/x$ in the limit $x \gg 1$ [3]. The form of the Brillouin function depends on the total spin moment of the particles since it takes account of the quantization of their orientations. However, for nanoparticles of the core size used here, it can be replaced by the Langevin function ($\coth x - x^{-1}$, the classical limit of the Brillouin function) with no loss of precision [3]. Accordingly, the magnetization data were fit to the Langevin function to derive N (the solute nanoparticle number

density), μ, and d. The measured magnetization is expressed in electromagnetic units (ergs/Gauss = 10^{-3} Joules/Tesla) per gram of iron (not iron oxide), units in general use in the current literature, and is readily converted to moment per unit volume using Avogadro's number and the known density of maghemite. The low- and high-field values of magnetization are given correctly by the Langevin function, independent of internal magnetic anisotropy and size polydispersity.

2.5.2. T_2 measurements

T_2 was measured with a Bruker Minispec PC 120/125/10 Vts NMR, at 10 and 20 MHz (0.23 and 0.47 T respectively), using the Carr–Purcell–Meiboom–Gill (CPMG) pulse sequence. The sample temperature was controlled (± 0.2°C) using circulating Fluorinert™ (3M Industrial Chemical Products Division, St. Paul, MN), and checked with a calibrated thermometer.

2.5.3. NMRD measurements and theory

The specialized instrumentation needed for measuring $1/T_1$ NMRD profiles of solvent protons, and the reproducibility and accuracy of such data have been described and reviewed in detail previously [8]. The $1/T_1$ NMRD profiles, taken at 5, 15, 25, and 35°C, span the approximate field range 0.2 mT to 1.2 T, corresponding to a proton Larmor frequency range of 0.01–50 MHz.

When comparing NMRD theory with experiment, it is initially assumed that the iron oxide cores are spherical (octahedral crystallite morphology is adequate), and that the oxidized starch polymer coating does not impede or restrict the diffusion of water, so that the diameter obtained from analysis of the NMRD profile gives d, the diameter of the iron oxide core. In the low-field (Curie) regime, $1/T_1$ and $1/T_2$ are determined by three parameters [3]: χ_C ($= N\mu^2/3kT$); r, the distance of closest approach of solute and solvent molecules (taken here as the sum of the radius of the iron oxide core ($d/2$) and the radius of a water molecule); and τ_S, the field-dependent re-orientational relaxation time of the magnetic moments of the particles. The relaxation rates also depend on the self-diffusion constant D of water molecules relative to solute. The value for pure water D_W is known to be appropriate for small paramagnetic agents [3], but questionable here (see below). In the high-field regime, reorientation of the solute moments becomes irrelevant, and only $N\mu^2$ and r determine $1/T_1$ and $1/T_2$. These two rates can be quite different; for particles of the size considered here, their ratio r_2/r_1 at 20 MHz is in the range 1.5–2. This ratio leads [3] to a value for r^2/D and therefore, d which, however, depends on assumptions about the value of D in the solute neighborhood. Knowing d and μ, M_{sat} ($= N\mu$) can be computed, and compared with the result from magnetization data. Since relaxation theory treats the nanoparticles as though their moments are localized at their centers, the value derived for τ_D, and therefore d, is that of the core particle plus the part of the coating that is impenetrable to water, unlike for magnetization data. Because, physically, M_{sat} is the volume density of the magnetic moment, one must take care to use only the volume of the magnetic regions of the nanoparticles when computing M_{sat} from μ.

Relaxation theory [3] also ignores the internal magnetic anisotropy of the particles (≈ 0.05 T), which only affects the predictions of theory in the transition from the low- to high-field regimes. This region is limited to about one decade of field and is essentially unimportant above 0.2 T (8 MHz). Below 0.01 T, in the Curie regime, nanoparticles behave as though they are magnetically isotropic [3], although τ_S can be influenced by anisotropy fields. Accordingly, we have not included data between 0.1 and 8 MHz when comparing NMRD measurements and theory. This procedure is similar to an earlier treatment of Mn^{2+}-protein systems [9], in which complications related to anisotropy of the electric crystal-field play a role analogous to magnetic anisotropy.

3. Results

3.1. Magnetization data

The data points, Fig. 1, show 25°C magnetization data for a solution of NC100150 (●) containing 2.57 mg/ml Fe, and for a solution of MION-46L (○) con-

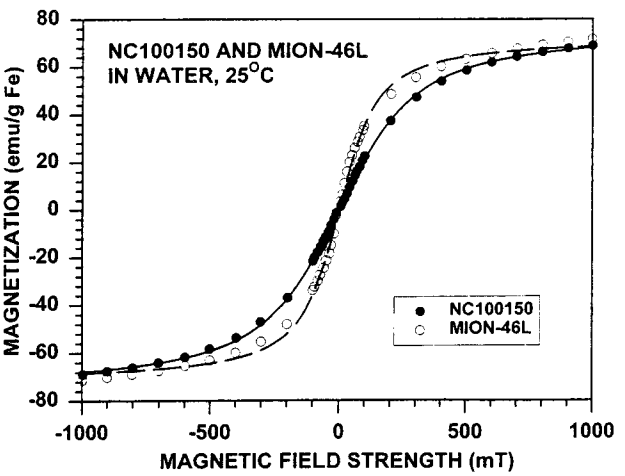

Fig. 1. Magnetization as a function of magnetic field B_0 for a 2.57 mg/cm^3 Fe solution of NC100150 (●) and a 7.18 mg/cm^3 Fe solution of MION-46L, at 25°C (○). The data points were fit to the Langevin function by a least-squares analysis, yielding the solid and dashed curves for NC100150 and MION-46L respectively.

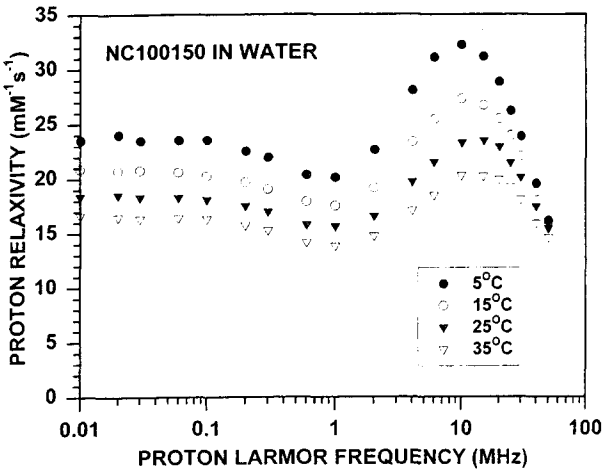

Fig. 2. $1/T_1$ NMRD profiles of a 15.0 μg/cm^3 Fe solution of NC100150, at 5 (●), 15 (○), 25 (▼) and 35°C (▽).

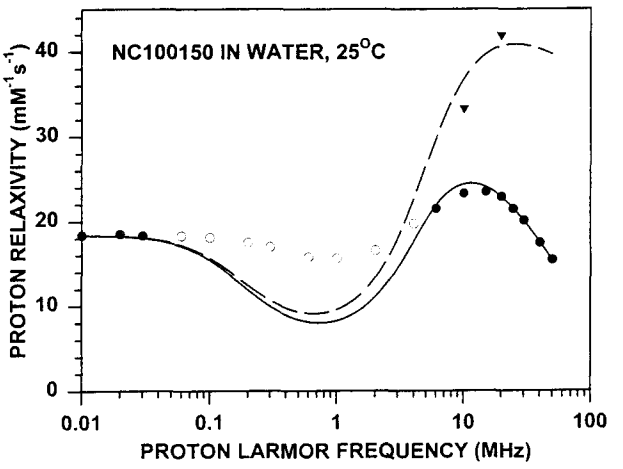

Fig. 3. Comparison of the measured $1/T_1$ NMRD profile, at 25°C, with outer sphere relaxation theory. The filled data circles are at fields for which the internal magnetic anisotropy of the nanoparticles should not compromise the accuracy of the theory (see text). The open circles were excluded from the comparison of data with $1/T_1$ theory [9]. Two measured values of $1/T_2$, at 10 and 20 MHz (▼) and at 25°C, are also shown. The solid curve shows the resulting theoretical $1/T_1$ profile and the dashed curve the $1/T_2$ profile *predicted* from this fit.

taining 7.18 mg/ml Fe. The solid and dashed curves are a least-squares fit of the Langevin function for NC100150 and MION-46L, respectively. For NC100150, the Langevin function is an excellent representation of the data over the entire field range. The quality of the fit, particularly at intermediate fields, is indicative of highly monodisperse iron oxide cores. Although the values of M_{sat} for both NC100150 and MION-46L are similar and consistent with the results reported earlier for MION-46 [7], the core size of MION-46L is significantly larger (by a factor of 1.3), consistent with the greater slope in the magnetization curve for fields less than 100 mT. In addition to being larger, the iron oxide cores of the MION-46L are not monodisperse, as indicated by the observable deviation of the fit from the data at intermediate fields (which also causes the value of M_{sat} obtained from the fitting procedure to be somewhat underestimated). The value of M_{sat} is about 60% of the value found for large maghemite samples [10], but is in essential agreement with the reported dependence of M_{sat} on size for maghemite nanoparticles [11]. For both of these samples, $4\pi\chi_C \ll 1$, thereby validating the assumption that sample demagnetization effects can be disregarded during the measurement of the magnetization curve [12].

3.2. NMRD data

Fig. 2 shows $1/T_1$ NMRD profiles of a 15.0 μg/cm^3 Fe (0.268 mM Fe) solution of NC100150, at 5 (●), 15 (○), 25 (▼) and 35°C (▽), expressed as relaxivity. Fig. 3 shows a fit of the 25°C $1/T_1$ NMRD profile, from Fig. 2, to outer-sphere relaxation theory. Two measured values of $1/T_2$ (▼), at 10 and 20 MHz and at 25°C, also expressed as relaxivity, are also shown. The filled data circles are for fields at which the internal magnetic anisotropy of the nanoparticles should not compromise the accuracy of the theory. From symmetry arguments, the anisotropy fields (~ 0.05 T) do not influence the validity of the theory as $B_0 \to 0$, where only τ_{S0} and τ_D are the only contributing correlation times [3]. At high fields, such that $B_0 \gg 0.05$ T (the range of the internal magnetic anisotropy), and the magnetization is nearing saturation, the internal anisotropy fields are comparatively small and can be ignored. It is only at intermediate fields, with data indicated by open circles, that the theory—which does not take internal magnetic anisotropy into account—may become inaccurate. Indeed, the expectation is that the profile would be broadened by ≈ 2 MHz, and its variation with B_0 evened out, much as is seen in Fig. 3. The open circles were excluded from the comparison of data with $1/T_1$ theory [3]. The solid curve shows the theoretical $1/T_1$ profile, a result of fitting the $1/T_1$ data to theory, and the dashed curve is the $1/T_2$ profile predicted from that fitting.

From the fit of the $1/T_1$ profile, and assuming for D its value for pure water at 25°C (2.50×10^{-5} cm^2 s^{-1}), we find a core diameter 1.3-fold greater than that obtained from the VSM data. This corresponds to a 2.2-fold greater particle volume than obtained from the magnetization data (Fig. 1), a large discrepancy which we attribute to breakdown of the assumption that D has the value of pure water. Accordingly, we use the values for M_{sat} and the core diameter obtained from the magnetization data and treat D and the thickness of a water-impenetrable coating as adjustable parameters in obtaining the fit to the NMRD data (Fig. 3). We find D

is about equal to that about half that of pure water at 25°C, and that there is a water-impenetrable coating (ostensibly a 'rind' of oxidized starch) such that comprises 18% of the core volume. The remaining 82% core volume consists of an iron oxide crystal. Additionally, we find that $\tau_{S0} = 2.17$ ns. From the ratio r_2/r_1 at 20 MHz, we find a value for d that is only 1% larger than that obtained from the fit of the $1/T_1$ profile, and adds further support to the magnetization data concerning the monodispersity of the core sizes. If the particle size distribution were not monodisperse, the value of d obtained from the r_2/r_1 ratio would be significantly greater than that obtained from the fit of the $1/T_1$ profile because the value of r_2 is very sensitive to larger core sizes [3]. As a technical aside, much of the initial increase in relaxivity above ≈ 2 MHz, Fig. 3, is due to a rapid increase in τ_S with B_0, as incorporated in relaxation theory for nanoparticles [3], and substantiates the sign of the field dependence of τ_S. This is also in accord with extensive calculations reported previously [13].

3.3. Photon correlation spectroscopy

PCS measurements give a 20°C translational diffusion constant for NC100150 that corresponds to a Brownian particle with hydrodynamic diameter 2.2-fold greater than that obtained from the VSM measurements. Thus, polymeric oxidized starch—extending from the oxidized starch rind into solvent and enhancing nanoparticle solubility—causes the volume of the composite particle to be a factor of 10-fold greater than that of the iron oxide core alone. This greater volume consists of mainly water; viscous interactions between polymer and solvent incorporate all this water in the diffusive mass of the nanoparticles [6].

4. Discussion

The major finding is that the three experimental techniques used here—magnetization curves, $1/T_1$ NMRD profiles, and PCS—give progressively larger values for the NC100150 nanoparticle diameter. However, only the result from magnetization data relates directly to the diameter of the magnetic core of the NC100150, without potential influence from the surrounding oxidized starch. As noted, these are thermodynamic data and should give the correct value for μ, or a volume average when the nanoparticles are polydisperse.

In NMRD experiments, the parameter actually measured is dynamic, with a correlation time τ_D given by r^2/D. Thus, the NMRD-derived value of the diameter would be reduced if D were reduced from the bulk solvent value. Such a reduction of the diffusivity of water molecules near the nanoparticle cores, but ostensibly outside a thin water-impenetrable rind of oxidized starch, is consistent with early work on the effective radius of gyration of linear polymers [6]. The NMRD measurements therefore can reveal much about the dynamics of water molecules entrained by the oxidized starch coating, provided the core size and magnetic moment are known from another technique.

A second aspect of the data also speaks to monodispersity: the excellent description of the magnetization data by the Langevin function in the intermediate field region. Significant polydispersity would distort the curvature of the data (the connection between the low- and high-field regimes), as could significant aggregation of the nanoparticles.

The observed values of M_{sat}, as noted, are about 60% of that of bulk maghemite, a result consistent with other observations [10,11]. The magnetic anisotropy constant of maghemite also appears different from its bulk value [14]. Perhaps this could have been expected, since the surface layer of an NC100150 nanoparticle comprises about 40% of the core maghemite molecules, and magnetic, chemical, and mechanical surface energetic have not been considered at all. Indeed, it is possible that the core size is stabilized by a balance of surface and volume energies, a potential advantage in synthesizing iron oxide nanoparticles with reproducible and relatively monodisperse core size.

The value of r_2/r_1, 1.83, at 25°C and 20 MHz (Fig. 3) is, to the best of our knowledge, the smallest ever reported for iron oxide nanoparticles at any temperature. For comparison, the published value of r_2/r_1 for MION-46 (an earlier preparation [7] of MION-46L) at 37°C and 20 MHz is 2.11. The r_2/r_1 ratio decreases with increasing temperature, and is equal to 1.69 at 35°C for NC100150. A low r_2/r_1 ratio is a significant advantage for these iron oxide nanoparticles as positive contrast agents for MRA. First, a greater degree of positive contrast can be attained since T_2 is not too short and T_2-effects are reduced. This is a benefit that becomes progressively more important at fields above 20 MHz, where clinical MRA is performed, since r_2/r_1 increases with increasing B_0 (cf. Fig. 3). Second, and perhaps more importantly, the value of r_2/r_1 at 20 MHz is a sensitive indicator of how strongly r_1 decreases with increasing field strength, as can be seen by comparison of the above r_2/r_1 ratios with the NMRD profiles at the corresponding temperatures (Fig. 3). At 20 MHz, the relaxivity at 25°C is significantly greater than it is at 35°C, but at 50 MHz, the relaxivities for both temperatures are similar. For clinical concentrations of iron oxides, the major contributor to the effective T_2 in blood arises from what is often called the susceptibility effect, an effect that requires a compartmentation of the

particles and that is independent of the r_2/r_1 ratio measured in water [15]. In the vasculature, the particles are compartmentalized in the extracellular space, which normally comprises about 60% of the total vascular space. Because very short echo times can now be used for clinical MRA, the contribution of susceptibility effects can be minimized, and it is the value of r_1 in water that mainly relates to the in vivo efficacy. Consequently, for two iron oxide preparations with identical values of r_1 at 20 MHz, the preparation with the highest r_2/r_1 ratio at 20 MHz will have the lower efficacy at higher field strengths. At fields relevant to MRA, where the only contributing correlation time is τ_D, the effect on relaxivity resulting from a decrease in temperature is similar to that resulting from an increase in core size [3]. Consequently, the small value of r_2/r_1 in comparison to that of MION-46L is consistent with their respective magnetization curves (Fig. 1); the core size of NC100150 is significantly smaller and more monodisperse than MION-46 and MION-46L. The advantage of NC100150 as a positive contrast agent for MRA is therefore a result of a core size that is optimal: it is large enough to cause its r_1 to be relatively high, and small and monodisperse enough to cause the r_2/r_1 ratio to be smaller than that for any other preparation reported to date.

In summary, it is possible to reconcile magnetization, $1/T_1$ NMRD, and PCS data on preparations of starch-coated maghemite nanoparticles, to provide a self-consistent characterization of their magneto-chemical properties. In doing so, one must consider the influence of the stabilizing organic surface coatings on the effective diffusivity of outer sphere water molecules, something not needed for smaller (uncoated) paramagnetic chelates. In this way, it has been possible to characterize a new preparation of magnetic nanoparticles, called NC100150, and confirm that their magnetic properties make them particularly suitable for MRA.

References

[1] Mandeville JB, Moore J, Chesler DA, Garrido L, Weissleder R, Weisskoff RM. Dynamic liver imaging with iron oxide agents: Effects of size and biodistribution on contrast. Magn Reson Med 1997;37:885–90.

[2] Knollmann FD, Böck JC, Teltenkötter S, Wlodarczyk W, Mühler A, Vogl ThJ, Felix R. Evaluation of portal MR angiography using superparamagnetic iron oxide. J Magn Reson Imaging 1997;7:191–6.

[3] Koenig SH, Kellar KE. Theory of $1/T_1$ and $1/T_2$ NMRD profiles of solutions of magnetic nanoparticles. Magn Reson Med 1995;34:227–33.

[4] Sjøgren CE, Johansson C, Nævestad A, Sontum PC, Briley-Sæbø K, Fahlvik AK. Crystal size and properties of superparamagnetic iron oxide (spio) particles. Magn Reson Imaging 1997;15:55–67.

[5] Koppel DE. Analysis of macromolecule polydispersity in intensity correlation spectroscopy: the method of cumulants. J Chem Phys 1972;57:4818–20.

[6] Tanford C. Physical Chemistry of Macromolecules. New York: John Wiley and Sons, 1961.

[7] Shen T, Weissleder R, Papisov M, Bogdanov A Jr, Brady TJ. Monocrystalline iron oxide nanocompounds (MION): physicochemical properties. Magn Reson Med 1993;29:599–604.

[8] Koenig SH, BrownIII RD. Field-cycling relaxometry of protein solutions and tissue: Implications for MRI. Prog NMR Spectrosc 1990;22:487–565.

[9] Bhattacharyya L, Brewer CF, Brown III RD, Koenig SH. Proton and deuteron magnetic relaxation dispersion sudies of Ca^{2+}–Mn^{2+}–lentil and Ca^{2+}–Mn^{2+}–pea lectin: evidence for a site of solvent exchange in common with Concanavalin A. Biochemistry 1985;24:4985–90.

[10] Chikazumi S, Charap SH. Physics of Magnetism. New York: John Wiley and Sons, 1964.

[11] Batis-Landoulsi H, Vergnon P. Magnetic moment of γ-Fe_2O_3 microcrystals: morphological and size effect. J Mater Sci 1983;18:3399–403.

[12] Bean CP, Livingston JD. Superparamagnetism. J Appl Phys 1959;30:120S–129.

[13] Aharoni A. Effect of a magnetic field on the superparamagnetic relaxation time. Phys Rev 1997;177:793–6.

[14] Mahmood SH. Magnetic anisotropy of fine magnetic particles. J Magn Magn Particles 1993;118:359–64.

[15] Fossheim S, Kellar KE, Fahlvik AK, Klaveness J. Low-molecular weight lanthanide contrast agents: evaluation of susceptibility and dipolar effects in red blood cell suspensions. Magn Reson Imaging 1997;15:193–202.